RT E JOURNAL

In-situ modification of material hardness for low-alloyed steels processed via PBF-LB/M – a view on process related microstructure

Maximilian Marschall [1,3,4]· Dominic Bartels [1-4] · Katja Tangermann-Gerk [1],
Stephan Roth [1,3,4] · Michael Schmidt [1-4]

1 Bayerisches Laserzentrum GmbH, 91052 Erlangen, Germany

2 Institute of Photonic Technologies (LPT), Friedrich-Alexander-University Erlangen-Nuremberg, 91052 Erlangen, Germany

3 Collaborative Research Center (CRC) 814 "Additive Manufacturing", 91052 Erlangen, Germany

4 Erlangen Graduate School in Advanced Optical Technologies (SAOT), 91052 Erlangen, Germany

https://doi.org/10.58134/fh-aachen-rte_2025_005

Zusammenfassung Das laserbasierte Pulverbettschmelzen von Metallen (PBF-LB/M) ermöglicht die Herstellung komplexer Bauteile mit dem Nachteil, dass nur ein Werkstoff verwendet werden kann. Im Zuge des In-situ-Legierens wird vorgemischtes Metallpulver mit zusätzlichem Kohlenstoff und verschiedenen Wolframkarbidgrößen untersucht. Härtesteigerung von 44 auf 55 HRC wurden bei einem niedrig legierten bainitischen Stahl durch Modifikation auf einen Kohlenstoffgehalt von 0,35 w.-% und 2,5 w.-% WC-Partikel, zur Partikelverstärkung, erreicht. Ziel ist die Erreichung der Härte im as-built Zustand für Wälzlageranwendungen. Um einen tieferen Einblick in die Aufhärtung und Mikrostrukturbildung während der In-situ-Modifikation zu erhalten, wird das Pulver mit Kohlenstoff-Nanopartikeln und WC-Mikropartikeln (0,9/2,5/8 µm) beschichtet. Die Proben wurden zunächst mit globaler Pulvermodifikation hergestellt, um Einflüsse der angestrebten Härte von Pulververteilungseffekten zu trennen. Danach wurden lokal in-situ modifizierte Proben hergestellt und auf ihre Härte und Mikrostruktur untersucht.

Abstract Laser-based powder bed fusion of metals (PBF-LB/M) enables to generate complex parts with the downside of using one material. In advance to local in-situ alloying, premixed metal powder with additional carbon and different tungsten carbide sizes is investigated. Hardness increases from 44 to 55 HRC were achieved with a low alloyed bainitic steel by modification to a carbon content of 0.35 w% and 2.5 w% of WC particles for particle reinforcement. As-built properties for bearing applications are desired. To get a deeper insight in the hardening and microstructure formation during in-situ modification, the powder is coated with carbon nanoparticles and WC microparticles (0.9/2.5/8 µm). Samples were built with global powder modification first, to separate influences of the aspired hardness from powder distribution effects. Then in-situ modified samples were built and investigated towards their hardness and microstructure.

Introduction and motivation

Within laser-based powder bed fusion with metals (PBF-LB/M) the predominantly used steel alloys are such to work well with the process conditions of high cooling rates. For this reason, low alloyed steels, especially for applications that require bainitic microstructures, are not a focus of PBF-LB/M yet [1]. Additionally, case hardening is required for lots of applications, preventing usage of as built parts. Having to work with powder material makes it easy to modify or mix them. This contribution takes a closer look at the hardening taking place during the process by modifying a bainitic steel with carbon black (C) and particle reinforcement with different tungsten carbide (WC) particle sizes. With the access to multiple hardening mechanisms and enhancing wear resistance, hardness is desired to be comparable to case hardened steel for bearings. The challenging tension field in process parameter dependent bainitic and martensitic microstructure within geometrical and temperature history influences makes these steels and modifications harder to be processed in PBF.

With all the degrees of freedom as well as in design and production, PBF-LB/M comes with the downside of using only one material for the part. Solutions with multi powder source PBF systems only address holistic material changes and don't operate on local alloy modification base [2]. On the road to a process that allows fine tuning the local alloy; like seasoning a dish on a plate as a tangible example– an achievable and desired alloy design and microstructure is crucial to investigate [3–5]. The first small step is to take a closer look at the fast alloying during the melt pool endures and the resulting microstructure. WC particles of different sizes and carbon black were chosen from the 'spice rack' of in-situ alloying in PBF-LB/M.

Materials and Methods

For the PBF-LB/M process, a commercially available powder was chosen. For low alloyed steel, only limited choices are available. DEW specialty steel GmbH & Co. KG offers a modified bainitic low alloyed steel, developed on the base of 1.7980 (18MnCrMoV4-8-7) and 1.7979 (18MnCrMoV6-4-8) with the name Bainidur® AM. A simplified short name is 22MnCrMoNiV5-4-10. The particle size is 20-63 µm. The as-built hardness is given with 44 HRC [6]. This alloy enables the comparison to low alloyed case hardening steels with bainitic microstructure in the field of bearing applications.

Table 1: Bainidur AM chemical alloy composition in wt. % from different sources; incoming inspection with ELTRA CS-i.

Source / Element	C	Si	Mn	Mo	Cr
Website [6]	0.22	0.8	1.4	1.0	1.0
Inspection certificate	0.26	0.7	1.3	1.0	1.1
Incoming inspection	0.2461 ±0.001	-	-	-	-

Tungsten carbide particles were provided by Kennametal Deutschland GmbH in three different fisher sub sieve sizes called WC 0.9/2.5/8.0 µm. For additional C, ASTM carbon black N550 nano particles (Harold Schold & Co. GmbH, Partenstein, Germany) were used.

Preliminary studies have shown, for desired application in bearing surfaces, a hardness of 58 HRC is desired. A total content of 0.35 wt. % C, available for alloying the matrix, was chosen according to martensite hardness of Just; together with 2.5 wt. % of WC particles and according to preliminary hardness measurements. For comparison, continuous cooling transformation (CCT) and time-temperature transformation (TTT) diagrams were calculated with JMatPro®.

All ingredients were dried for 12 hours at 100 °C in a vacuum oven. The modified powder was premixed for global in-situ alloying. Glass spheres of 1 mm were used as mixing agents while blending the powder with the additional alloying ingredients for two hours in a tumbler mixer. Afterwards the powder was sieved at 125 µm. The desired carbon content modification was checked after sieving with an ELTRA CS-i analyzer for the powder materials. It reached an overall carbon content of 0.475-0.495 wt. %, including the carbon of WC, which fits the calculations of 0.35 wt. % C and 2.5 wt. % WC. The adhesion of the added carbon black and WC on the Bainidur host particle surface can be seen in Fig. 1. As the fraction of added WC is the same in all mixtures, the spreading on the surface highly depends on the particle size of the WC. Smaller WC results in better and more homogenous coverage. Agglomerates may occur but are minimized with the usage of the glass mixing agents.

Optical emission spectroscopy (OES) was performed with a Bruker Q4 TASMAN OES for tungsten and carbon content measurements of the processed samples.

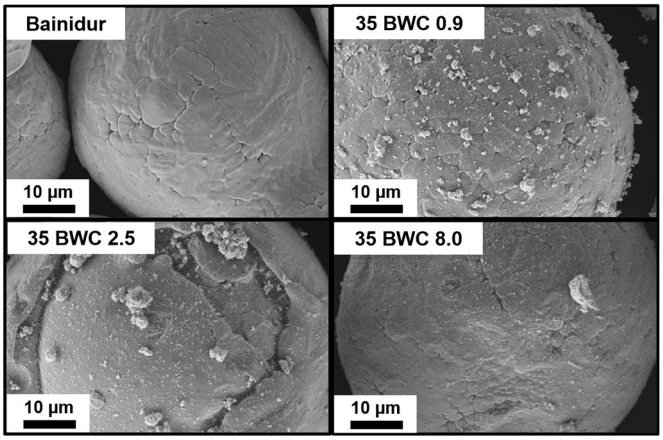

Fig. 1: powder mixture results with superficial adhesions of carbon black and WC particles in different sizes.

The material was processed on an Aconity Mini PBF-LB/M machine. The parameter range was defined via statistical evaluation of a parameter screening to set up a full factorial parameter study. This enables to react to powder modification dependent parameter changes. The ranges are 100/175/250 µm for hatch distance, scanning speed 750/1375/2000 mm/s and laser power in the focus of a gaussian beam 100/300/500 W. The laser spot size was 71.9 µm with a Rayleigh length of 2.3 mm. Layer height was set to 60 µm due to particle size. The scanning rotation starts at angle of 22° and 67.5° rotation increase to avoid self-repeating structures on short intervals according to Fibonacci's law for plant leaves. The last layer was oriented to have the scanning direction perpendicular to the image plane of the metallographically prepared samples. The last layer hatch was oriented perpendicular to the image plane of the metallographically prepared samples. The sample position was first randomized and then fixed for all built jobs.

For the multi material built job, the powder feeder cylinder was prepared to contain vertically stacked layers of Bainidur / modified Bainidur / Bainidur relating to the approach of Huber to study the material grading on the layer border [7]. Each layer was prepared with a stamping device and spirit level to achieve conformity with the recoating level. This enables material to change within few layers.

The relative sample density of polished cross sections was evaluated with the ImageJ plugin package Fiji with Otsu method for 8-bit color thresholding. Hardness was measured with HV10 method and converted to HRC. Five indents were done, two in the upper 500 µm layers, one in the transition zone and two in the bulk. Etched samples were prepared with 3 % Nital.

Sample labeling will be according to carbon measurement (0.25 wt.%) 25B for Bainidur and (0.35 wt.%) 35BWC0.9/2.5/8.0 for increased carbon and tungsten carbide modification for the different particle sizes.

Results and Discussion

From the full factorial parameter study, effects on the required energy input for dense samples were extracted. In the following the influence of the powder modification with carbon and tungsten carbide on density, hardness and microstructure will be described. Afterwards an in-situ modified multi material sample will be discussed and evaluated with EBSD whether the additional carbon takes part in the alloying of the steel.

CCT calculations

Depending on the inspected and modified carbon content, the hardness is influenced. Assuming high cooling rates prevailing in PBF-LB/M without further preheating, formation of martensite and bainite is dominating the microstructure. Perlite and Ferrite is suppressed for this low alloyed steel. The following Table 2 includes the simulated hardness that is achievable for a martensitic microstructure in the given composition based on the Bainidur AM powder. The results for 0.22-0.26 wt.% C is included because of the different alloy information from Table 1. Ongoing all modifications were targeted to 0.35 wt.% C for the matrix alloy before interacting with the WC particles, which can, depending on process parameters, provide locally additional carbon in solid solution

Table 2: Theoretical achievable hardness with martensitic microstructure in dependence of modified carbon content in Bainidur AM according to JMatPro® calculations without WC particles.

Carbon content in wt.%	0.22	0.24	0.26	0.35	0.4
Max. hardness in HRC	47	49	51	55	57
Martensite Start in °C	346.8	339.3	331.9	298.7	280.6
Martensite End in °C	231.2	223.0	214.9	178.3	158.3

Influence of C and WC on relative density

The modification with WC and C resulted in higher relative densities with the same parameter set, according to Fig. 2. Hausner ratio kept the same around 1.14 despite the

powder modifications, therefore powder bed density effects, which are often discussed in polymer powder bed, can be excluded here.

The average density increase was about 5 % relative to the unmodified Bainidur, while the standard deviation of the relative density increase over all samples was in the same region in all modifications taken. Thus, this increase in density was not significant. While working in a parameter field that produces dense samples, modified/unmodified reached the same density within standard deviations. Leaving this field, it must be mentioned that this influence was significant and increased the density in certain cases over 20 % as to be seen in Fig. 2. That indicates that the modified powder requires less nominal energy input to reach dense conditions compared to the original powder or laser absorptivity was enhanced. The best results were achieved with 35 BWC 2.5.

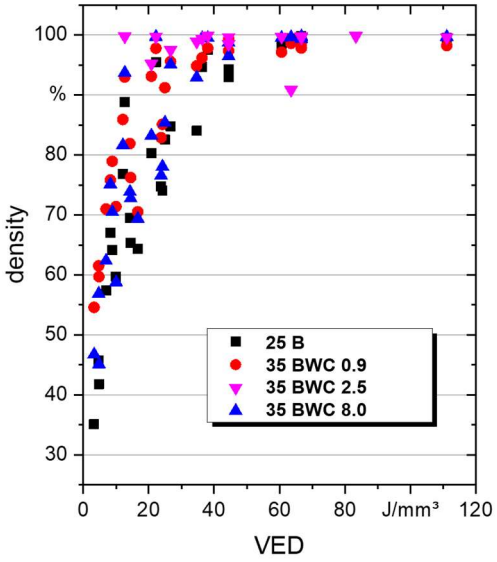

Fig. 2: Sample density over volume energy distribution (VED).

Influence of C and WC on hardness

For the 25 B (Bainidur) samples the specified hardness was reached with 43.9 ± 0.4 HRC. This also indicates having a stable process parameter set that achieves the datasheet values for the material. Within the measurement inaccuracy there was no difference between the upper surface layers to the in-situ heat treated bulk. As the alloy is designed to have an enlarged bainite phase in the time-temperature transformation diagram (TTT), the formation of a bainite like microstructure is ensured even with the high cooling rates in PBF at surfaces. The temperature of the building plate was tracked during the process and showed a stable temperature of 220 °C already after few first layers. The bulk temperature in the samples is higher but not exceeding the bainite phase area temperature known for similar bainitic steels [8]. The investigated microstructure formation was already discussed in [9] and prevailed bainitic or bainite-like, despite the complex influences of microstructure formation in PBF. Formation of upper and lower bainite could be observed.

With additional C and WC, a change in hardness is observed, summarized in the left Fig. 3. Not only the average increased to 55.1 HRC, but standard deviation also increased. Taking a closer look at the single indents, the hardness of the bulk is at 50 HRC while going

up to 52 in the transition zone. But the surface layers exceed 62 HRC. This was achieved with 35BWC8.0. The usage of WC2.5 resulted in 54.7 ± 5.1 HRC, WC0.9 in 52.3 ± 1.3 HRC with significant lower deviation between the surface and the bulk. Microstructure investigations will reveal the changes and local dependencies of the hardness despite homogenous distribution of the alloying elements. Illustrated in Fig. 3 on the right is a WC8.0 particle that has a distinct solution and diffusion zone. The dimension of this zone suggests, that the WC0.9 particles will not be able to prevail a stable core and dissolve completely. Remaining cores of WC0.9 could not be found in SEM analyses. This indicates, why the hardness is lower compared to the modifications with bigger sized WC particles. A stable WC content was measured in EDX, also at high distance to visible WC particles, with 1.5 %. Over all tungsten content measured via OES was 2.04 %. Grain boundaries are W enriched shown by EDX and the Angle-selective Backscatter (AsB) detector in Fig. 4. It is unlikely that the WC can be molten at process temperatures for the low alloyed steel, therefore diffusion and solution must be the dominant mechanisms of WC interacting with the matrix, also addressed from Kang et al. [10]. Having a closer look to the equilibrium solubility of WC, iron as solidified ferrite can only solve a small amount of WC, also depending on its carbon content [11]. As we have a microstructure dominated by bainite, resulting in a main fraction of carbon being bond in small cementite precipitates, the solved carbon in the remaining ferrite is lower than the mean carbon content. But still the solvable equilibrium tungsten content in ferrite is about max. 0.2 wt.% [11], resulting in an accumulation of WC at the ferrite grain boundaries. This effect can be seen in Fig. 4 as tungsten emerging the cellular grains, without the presence of WC particles or remaining diffusion zones and particle cores like in Fig. 3 on the right side. This is the result of a far-reaching distribution of WC from its origins as a particle throughout the melt pool and recurring remelting.

Carbon content of the processed samples via OES was unchanged for the unmodified 25 B. The built samples of the modified powders show a general loss of carbon of 0.01 % total compared to the initial characterization in materials and methods and a pure tungsten content of 2.04 %.

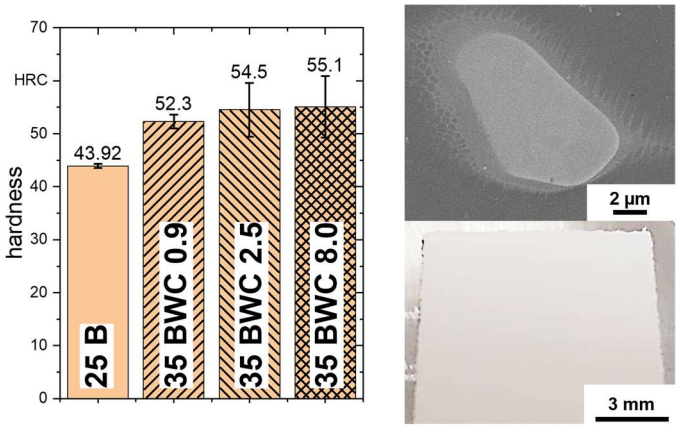

Fig. 3: left: Average sample hardness of Bainidur in dependency of C and WC alloying; upper right: solution and diffusion zone around a WC8.0 particle, SEM with AsB detector; lower right: overview of 35WC2.5 sample.

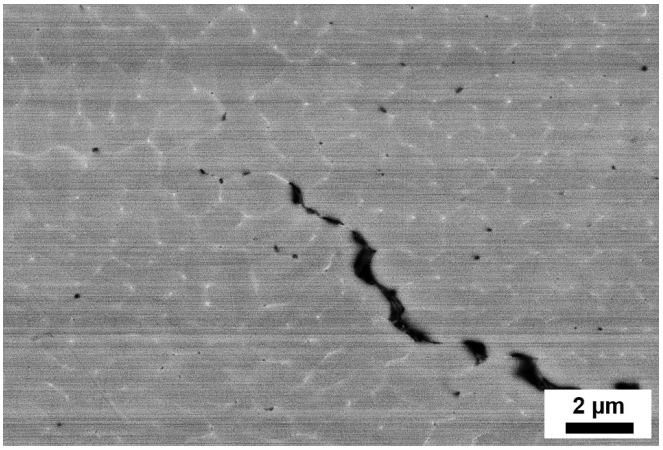

Fig. 4: SEM image with AsB detector, cellular grains in 35 BWC 2.5 with brighter grain boundary areas due to tungsten enrichment.

Microstructural changes in as-built state

As the full determination of phases, especially in bainitic steels, would exceed this contribution [12,13], the microstructure is characterized by the local sample hardness and images of Nital etched samples with optical microscope.

Depending on the inspected area, different microstructure can be found. With the chosen scanning rotation increase of 67.5° per layer, the single weld tracks or layers are no longer pronounced visible in the bulk sample compared to Bartels et al. [9]. In Fig. 5 different but inherent homogenous microstructures can be seen. The images Fig. 5 a) and b) are from 25B, c) and d) from modified powder. Additionally, a) and c) are in the upper layer region of the built sample and b) and d) representing the bulk. It can be clearly seen, that the modification with C and WC leads to a distinct martensite formation in the upper layers. While first forming a martensitic austenitic microstructure, the unavoidable heat treatment during process provides tempering the martensite and the transformation to bainite. Having a look at 25B in a), there is no dominating martensitic microstructure despite the same high cooling rates that dominate PBF-LB/M. Only with a higher fraction of retained Austenite compared to underlying layers. Going into the bulk, the prominent microstructure does not change besides tempering effects. This can also be seen in the low hardness deviation between the surface layers and the bulk, where else the 35BWC has a significant drop in hardness from the martensitic regions to the stable but lower hardness of the in-situ heat treated bulk, like already mentioned in 0.

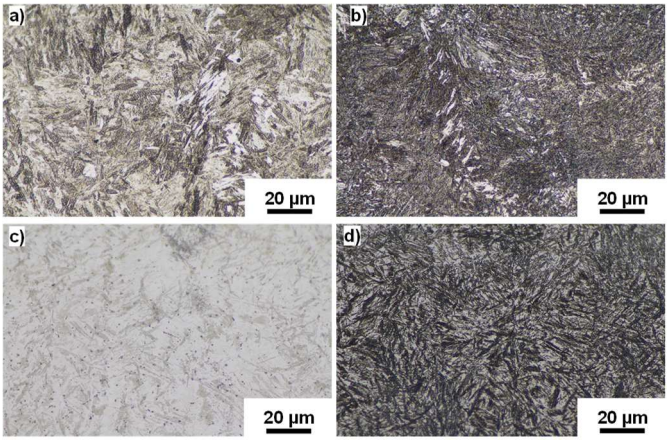

Fig. 5: Microscope images of a,b) 25B and c,d) 35BWC2.5; a) and c) are at the cubic sample upper surface, b) and d) are representative for the rest of the sample volume.

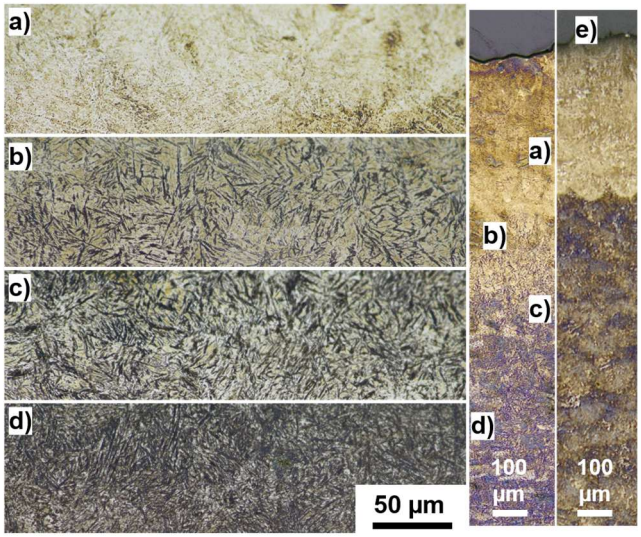

Fig. 6: Microstructure development in C+WC modified Bainidur from a) last weld tracks (up to 500 µm depth) over the transition zone b)+c) to the bulk microstructure in d); on the right a correlating overview and e) 25B overview for reference.

While in the unmodified steel we can see a sharp transition between the microstructure of the last weld tracks and the bulk beneath, in the modified powder samples an enlarged transition zone is observable, that exceeds the region of the last weld. This microstructural development from surface layer to bulk is illustrated in Fig. 6. This transition zone reaches about 1000 µm deep until there is no more obvious change in microstructure. Expressing in different hardness like already pointed out, horizontally thin parts will develop significant different mechanical properties compared to the bulk or/and compared to the stable microstructure of the base alloy.

Multi material sample with in-situ modification

As the sample was built with horizontal stacked material changes, a closer look to the material transition zone is necessary. The achievable properties are now known from the unmodified and global modified powder built jobs. As seen in 0 the modification results in slightly denser samples compared to the same VED parameter sets to the Bainidur. The

samples were built with an interpolated parameter set from Fig. 2 at 55.5 J/mm³ with scanning speed of 750 mm/s, a powder of 300 W, 60 µm layer with 120µm hatch and laser beam in focal plane. The sample size is 10x10x12 mm. They reached a total rel. density of 99.9 %. Fig. 7 shows an etched cross section of a sample that reveals the different microstructure and correlating hardness of the modified area. It can be seen that despite the different hardness and relative sharp transition zone there are no bonding defects and cold cracks. The transition zone measures about the same depth like the welding depth of the last weld tracks on the surface of the sample and is therefore dependent of the process parameters. In this case it is about 300 µm that can be measured between the representative microstructures that are shown in Fig. 5 b) and d), between bainite and martensite like area. Having the change in microstructure in less range than the welding depth of this parameter set, this can be called a sharp transition. But the resulting hardness is not the same, as investigated in the global modified samples from Fig. 3. Having a look at the deviations also the unmodified Bainidur is about 2 HRC lower than expected. The mean value of the modified section is 4.5 HRC lower. As significant decarburization was not measurable in the experiments with the global modified powders, it is not expected to be the main reason for this drop in hardness. OES measurements show stable carbon content in the unmodified Bainidur 25 B sections with 0.24 %, which fits the inspection of the powder. The modified section turned out to have a carbon content of 0.45 % and a tungsten content of 1.89 %. Both values are lower than the global modified samples 35 BWC 0.9/2.5/8.0. As decarburization could be excluded for now, because 25 B was unchanged, the reason for this loss of most likely WC particles has to be the reuse of the powder. During the sieving process WC particles were detached from the Bainidur host particle.

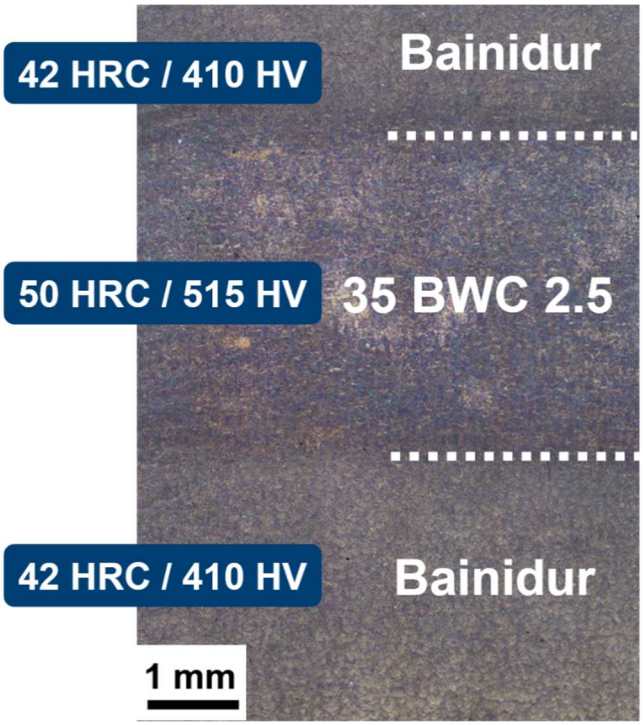

Fig. 7: Overview of in-situ modified layer sandwiched by unmodified Bainidur with resulting hardness; sample was etched with Nital.

Investigations with EDX show a relatable content of 1.7 % of tungsten distributed in the modified section. No remaining particles were in the measurement field. This also hints a slight loss of the WC particles from the second sieving step for the reuse of the powder. Remaining WC particles or cores were rarely found like in the WC 0.9 samples from the global alloying, but WC 2.5 was used here. The decrease in hardness in both modified and unmodified sections indicate, that the microstructure was in-situ heat treated more with the bigger sample volume. This correlates well to the hardly to find WC particles and the homogenous distributed tungsten in the EDX. Known from literature for slower laser processes like direct energy deposition, the energy input and melt pool duration defines the degree of dissolution of the primary WC particles in the metal alloy matrix [14]. And of course the smaller the particles are, the faster they are able to be solved [15]. Fig. 8 supports this hypothesis with its homogenously distributed tungsten from an EDX measurement that was executed simultaneously to the EBSD. The other elements are within the expected range for the Bainidur AM alloy according to OES measurements and the composition by DEW [6].

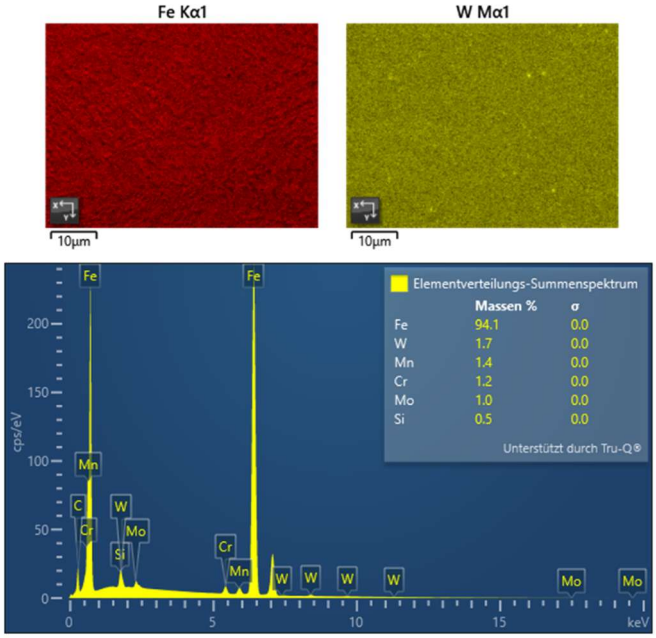

Fig. 8: EDX (simultaneous to EBSD) measurement within the modified section of Fig. 7 with homogenous tungsten distribution.

Taking a closer look at the microstructure of the sections. A distinct transition zone could not be found In a way to be visualized in SEM and EBSD images. Therefore, the focus will be on the microstructure within the two sections of Bainidur AM (25 B) and the modified one with higher carbon content and WC particles with 2.5 µm diameter (35 BWC 2.5). In the EBSD inverse pole figure maps a distinct orientation can not be seen, correlating to the Fibonacci angle of hatch rotation. In Fig. 9, within smaller superstructures relating to the weld root cross sections of the associated hatch direction, upward facing grain growth can be seen. But this is a very locally occurring pictural analysis. On the upper right side of both images the growth direction is not this pronounced. The analysis spots were intentionally chosen to show similar overlapping hatch orientations, but taking the scale bar into account, there would only fit one weld track perpendicular to the image plane in

full width. Resulting from the hatch, layer height and welding depth, only sections of 10-20 µm height last in an inherent homogeneous orientation. In general, both orientation maps are similar and there is no grain fining visible. From these measurements the feret diameter is 1.12 µm for the 25 B and 1.27 µm for 35 BWC 2.5, but the difference is within the standard deviation of the evaluation. It was expected to be at the same level or even, that the additional particles in 35 BWC 2.5 serve as nucleating agents and reduce the grain size. Such effect was shown by Becker et al. when two powders were blended and processed to achieve the same chemical composition like a pre alloyed third powder [16].

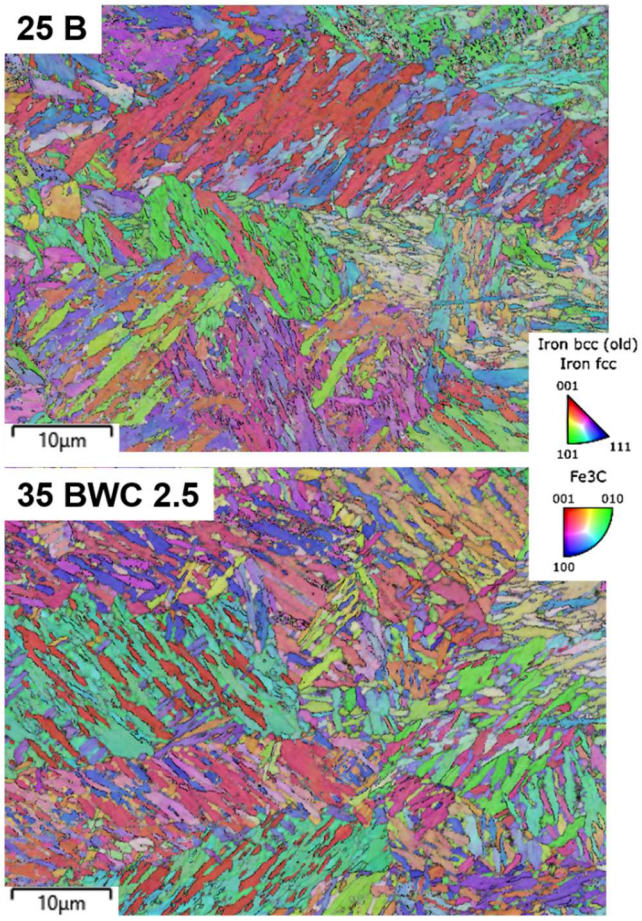

Fig. 9: EBSD grain orientation map in Y-direction based on the inverse pole figure of the sample in Fig. 7 in the resp. material sections.

But to be seen in Fig. 10 is the difference in austenite and ferrite fractions in the microstructure. The retained austenite doubled from 5.3 % to 11.9 %. Not going into detail about the bainite/cementite because of the 12 % zero solutions as small areas believed to be mostly this phase in both cases. Having the in-situ modification mostly done with carbon, as the WC goes only into diffusion-controlled solution because of its chemical and thermal stability, the biggest influence on the microstructure is the phase stability change within the nickel-equivalent. It is influenced by carbon with a factor of 22 and stabilizes the austenite phase [17]. This will only be possible when the carbon is available for the alloying and is no longer persisting as particles or agglomerates. To close the arc to the initial goal about the in-situ modification and alloying process, it could be shown, that the carbon is fully available for alloy formation and even the WC hard particles are able to be

solved, even though this is not completely intended as they should serve as precipitation hardening particles with unsolved cores to achieve the final desired hardness.

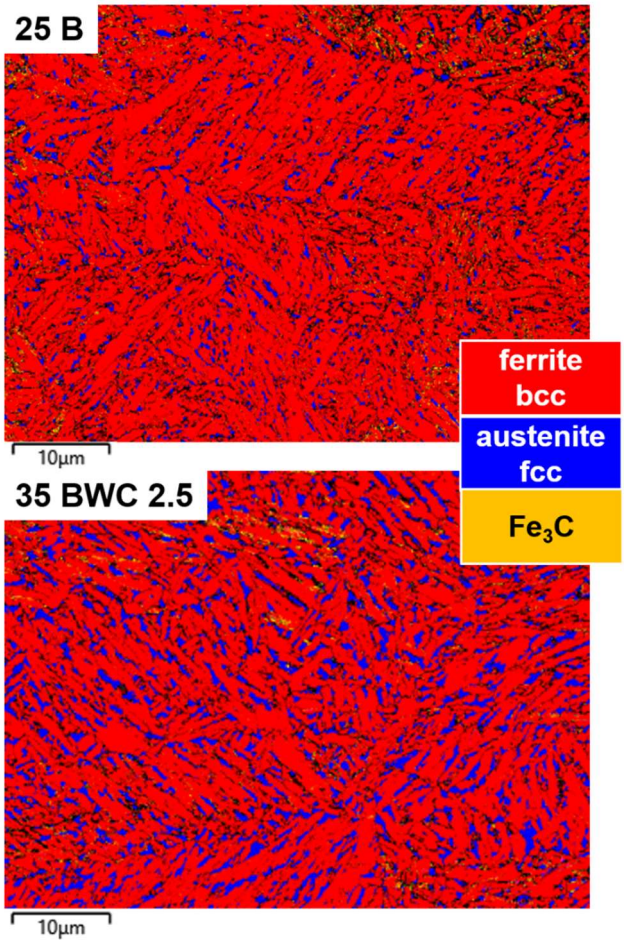

Fig. 10: EBSD phase analyses map of the sample in Fig. 7 in the resp. material sections and same position to Fig. 9.

Conclusion and outlook

Low alloyed bainitic steel was enhanced via global in-situ modification with carbon and WC particles. A multi material sample was built with the investigated compositions. By adding carbon black and WC particles, density increased within the same process parameters. Within the used WC particle sizes, a trend was observed for higher sample density corelated to smaller WC particles. Modification with WC8.0 resulted in higher hardness. Particles showed good interconnection to the steel matrix material and developed distinct diffusion zones. Due to remelting of underlying layers and in-situ heat treatment, the highest hardness was achieved at the surface and drops beneath the upper layer welding depth to a stable value for the rest of the sample. This pronounced hardness deviation from surface to bulk was not observable for the unmodified Bainidur.

It could be seen that the elaborated process parameters and this concentration of the WC particles do not create bonding defects because of the pronounced diffusion zone and solvability. But from these results a particle size in between 2.5 and 8 µm is desired to

obtain an unsolved particle core for the precipitation hardening effect. The multi material part with the in-situ modified sandwich layer was not able to reach the same hardness as the global powder composition did in the parameter studies with smaller samples. Reuse of modified powder resulted in a small loss of WC content. Because of the recurring subsequent melting and in-situ heat treatment, the fraction of solved or diffusive mobile WC increased with sample size and reduced the as-built hardness. For real parts the chosen WC particle size must be considered depending on the local thermal history of the built part and the carbon content might be chosen higher to achieve the desired hardness for the bearing application.

Future studies will deal with the effects of post process heat treatment and address deeper insights into the risks of cold and hot cracking during in-situ modification. It will include EBSD investigations into bainite and martensite formation within the fast process of alloy modification and formation in PBF-LB/M. This contribution is the first step towards a local in-situ alloying process to enable as built material properties to suit for bearing applications. In advance, the complex microstructure forming must be controlled before being able to apply it on a dedicated local safety relevant area of an additive manufactured part.

Acknowledgement

The authors gratefully acknowledge funding of the Collaborative Research Center 814 (CRC 814), sub-project T5, by the German Research Foundation (DFG)-Project No. 61375930 and of the Erlangen Graduate School in Advanced Optical Technologies (SAOT) by the Bavarian State Ministry for Science and Art. And Kennametal Deutschland GmbH for providing a variety of WC particles.

Contributions

Conceptualization MM; data curation MM; formal analysis MM; methodology MM; metallography MM,KT; supervision DB,SR,MS; writing-original draft MM; writing-review and editing MM, DB,SR,MS

References

[1] Bajaj P, Hariharan A, Kini A, Kürnsteiner P, Raabe D, Jägle EA. Steels in additive manufacturing: A review of their microstructure and properties. Mater Sci Eng A 2020;772:138633. https://doi.org/10.1016/j.msea.2019.138633.

[2] Additive Fertigung mit Multimaterial | Schaeffler Special Machinery n.d. https://www.schaeffler-special-machinery.de/de/produkte/additive-fertigung/ (accessed February 20, 2024).

[3] Mosallanejad MH, Niroumand B, Aversa A, Saboori A. In-situ alloying in laser-based additive manufacturing processes: A critical review. J Alloys Compd 2021;872:159567. https://doi.org/10.1016/j.jallcom.2021.159567.

[4] Schmitt M, Gottwalt A, Winkler J, Tobie T, Schlick G, Stahl K, et al. Carbon Particle In-Situ Alloying of the Case-Hardening Steel 16MnCr5 in Laser Powder Bed Fusion. Metals 2021;11:896. https://doi.org/10.3390/met11060896.

[5] Hesselmann M, Fechte-Heinen R, Mädler L, Steinbacher M, Toenjes A. Smart-Alloying – Liquid in-situ re-alloying in additive manufacturing. Addit Manuf 2024;80:103988. https://doi.org/10.1016/j.addma.2024.103988.

[6] Bainidur AM - dew-powder.com n.d. https://www.dew-powder.com/additive-fertigung/bainidur-am (accessed February 20, 2024).

[7] Huber F. In-situ Alloy Formation of Refractory Metal Alloys by Laser Powder Bed Fusion (PBF-LB/M). Friedrich-Alexander-Universität Erlangen-Nürnberg, 2024.

[8] Bainitische Stähle. SSG n.d. https://swisssteel-group.com/de/produkte/edelbaustahl/bainitische-staehle (accessed April 4, 2024).

[9] Bartels D, Novotny T, Mohr A, van Soest F, Hentschel O, Merklein C, et al. PBF-LB/M of Low-Alloyed Steels: Bainite-like Microstructures despite High Cooling Rates. Materials 2022;15:6171. https://doi.org/10.3390/ma15176171.

[10] Kang N, Ma W, Heraud L, El Mansori M, Li F, Liu M, et al. Selective laser melting of tungsten carbide reinforced maraging steel composite. Addit Manuf 2018;22:104–10. https://doi.org/10.1016/j.addma.2018.04.031.

[11] Pavlina EJ, Speer JG, Van Tyne CJ. Equilibrium solubility products of molybdenum carbide and tungsten carbide in iron. Scr Mater 2012;66:243–6. https://doi.org/10.1016/j.scriptamat.2011.10.047.

[12] Zajac S, Schwinn V, Tacke KH. Characterisation and Quantification of Complex Bainitic Microstructures in High and Ultra-High Strength Linepipe Steels. Mater Sci Forum 2005;500–501:387–94. https://doi.org/10.4028/www.scientific.net/MSF.500-501.387.

[13] Ståhlkrantz A, Hedström P, Sarius N, Borgenstam A. Revealing the Unexpected Two Variant Pairing Shifts Due to Temperature Change in a Single Bainitic Medium Carbon Steel. Metall Mater Trans. 2021;52:4546–57. https://doi.org/10.1007/s11661-021-06408-0.

[14] Przybyłowicz J, Kusiński J. Structure of laser cladded tungsten carbide composite coatings. J Mater Process Technol 2001;109:154–60. https://doi.org/10.1016/S0924-0136(00)00790-1.

[15] Bartels D, Novotny T, Hentschel O, Huber F, Mys R, Merklein C, et al. In situ modification of case-hardening steel 16MnCr5 by C and WC addition by means of powder bed fusion with laser beam of metals (PBF-LB/M). Int J Adv Manuf Technol 2022;120:1729–45. https://doi.org/10.1007/s00170-022-08848-3.
[16] Becker L, Lentz J, Benito S, Cui C, Ellendt N, Fechte-Heinen R, et al. A comparative study of in-situ alloying in laser powder bed fusion for the stainless steel X2CrNiMoN20-10-3. J Mater Process Technol 2023;318:118038. https://doi.org/10.1016/j.jmatprotec.2023.118038.
[17] Bargel H-J, Schulze G. Werkstoffkunde. 12. Auflage. Springer Berlin Heidelberg; 2018.

Contact

Maximilian Marschall, M.Sc.
Bayerisches Laserzentrum GmbH
Konrad-Zuse-Str. 2-6
91052 Erlangen
E-Mail: m.marschall@blz.org